Predictive Binding of β-Carboline Inverse Agonists and Antagonists via the CoMFA/GOLPE Approach

Michael S. Allen,† Anthony J. LaLoggia,† Linda J. Dorn,† Michael J. Martin,† Gabriele Costantino,‡ Timothy J. Hagen,§ Konrad F. Koehler,*,∥ Phil Skolnick,⊥ and James M. Cook*,†

Department of Chemistry, University of Wisconsin—Milwaukee, Milwaukee, Wisconsin 53201, Laboratorio di Chemiometria, Dipartimento di Chemica, Università degli Studi, Perugia, Italy, Department of Chemistry and Drug Design Section, Searle Research and Development, Skokie, Illinois 60077, and Laboratory of Neuroscience, National Institute of Diabetes and Digestive and Kidney Diseases, National Institutes of Health, Bethesda, Maryland 20892

Received March 26, 1992

The synthesis and affinities of six new 3-substituted β-carbolines (6–10, 12) for the benzodiazepine receptor (BzR) are described. These analogs were used both to probe the dimensions of the hydrophobic pocket in the benzodiazepine receptor and to test the predictive ability of a previously reported 3D-QSAR regression model. Of the new analogs synthesized, the γ-branched derivatives (isobutoxy, 7, IC_{50} = 93 nM; isopentoxy, 9, IC_{50} = 104 nM) display significantly higher affinity for the BzR than either the β-branched (*sec*-butoxy, 6, IC_{50} = 471 nM; *tert*-butyl ketone, 12, IC_{50} = 358 nM) or δ-branched (isopentoxy, 8, IC_{50} = 535 nM) analogs. An exception to this rule is the γ-branched 3-benzyloxy derivative 10 (IC_{50} > 1000 nM) which appears to have a chain length that is too long to be accommodated by the BzR. The standard error of prediction for these six new β-carbolines using the original regression model is significantly lower than the standard error estimate of the cross validation runs on the training set, hence the predictions made using this model are much better than expected. In order to obtain more credible predictions, a new procedure called GOLPE (generating optimal linear PLS estimates) was used to eliminate irrelevant electrostatic and steric descriptors from the regression equation. A substantial reduction in the standard error estimate resulted. The predictions from this new regression equation were somewhat less accurate than the ones obtained with the original regression equation; however the standard error of prediction and the standard error estimate are in much closer agreement. Finally, to probe the effect that the quality of the steric and electrostatic potentials has on 3D-QSAR analyses, the semiempirical MNDO//PRDDOE geometries and Mulliken charges used in the original analyses were replaced with ab initio 3-21G//6-31G* geometries and electrostatic potential fit charges. A modest decrease in the standard error estimate and increase in cross validated R^2 resulted.

Introduction

Cognitive enhancing agents targeted against age-associated memory impairment,[1-5] as well as for the enhancement of general memory-learning,[6-8] have attracted a great deal of recent attention. For example, it was reported that 2-(5-methylthien-3-yl)-2,5-dihydro-3*H*-pyrazolo[4,3-c]quinolin-3-one (1) may be useful for activating depressed brain function.[9] In addition, the benzodiazepine receptor (BzR) inverse agonist methyl-β-carboline-3-carboxylate (2, βCCM) was found to enhance animal performance in three different tasks used to investigate memory and learning in three separate animal models.[6,7] Moreover, ethyl 5-isopropoxy-4-methyl-β-carboline-3-carboxylate (ZK-93426) has been shown to increase alertness and improve attention in man.[8] In a related area, there is interest in identifying compounds that have the ability to reverse the effects of barbiturate-induced central nervous system (CNS) depression or overdose.

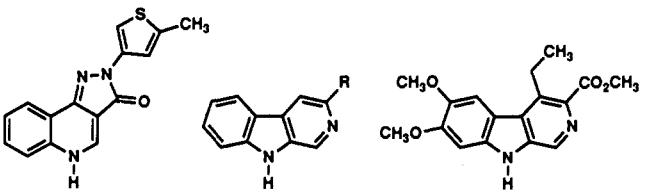

1 2; R = CO_2CH_3 4; R = CH_2OH 5; R = OCH_2CH_3 3

Although effective antagonists have been developed to counteract deleterious effects of opiates and benzodiazepines, efforts to discover such compounds for treatment

† University of Wisconsin—Milwaukee.
‡ Università degli Studi.
§ Department of Chemistry, Searle Research and Development.
∥ Drug Design Section, Searle Research and Development; inquiries concerning the computer modeling aspects of this paper should be directed to this author.
⊥ NIH.

(1) Crook, T. H.; Johnson, B. A.; Larrabee, G. J. In *Methodology of the Evaluation of Psychotropic Drugs*; Benkert, O., Maier, W., Rickels, K., Eds.; Springer-Verlag: Berlin, 1990; pp 37–55.
(2) Crook, T. H.; Tinklenberg, J.; Yesavage, J.; Petrie, W.; Nunzi, M. G.; Massari, D. C. Effects of Phosphatidylserine in Age-Associated Memory Impairment. *Neurology* 1991, *41*, 644–649.
(3) McEntee, W. J.; Crook, T. H. Age-Associated Memory Impairment: a Role for Catecholamines. *Neurology* 1990, *40*, 526–530.
(4) Bartus, R. T. Drugs to Treat Age-Related Neurodegenerative Problems. *J. Am. Geriatr. Soc.* 1990, *38*, 1–16.
(5) Altman, H. J.; Normile, H. G. What is the Nature of the Role of the Serotonergic Nervous System in Learning and Memory? Prospects for Development of an Effective Treatment Strategy for Senile Dementia. *Neurobiol. Aging* 1988, *9*, 627–638.
(6) Venault, P.; Chapouthier, G.; Prado de Carvalho, L.; Simiand, J.; Morre, M.; Dodd, R. H.; Rossier, J. Benzodiazepine Impairs and β-Carboline Enhances Performance in Learning and Memory Tasks. *Nature (London)* 1986, *321*, 864–866.
(7) Venault, P.; Chapouthier, G.; Prado de Carvalho, L.; Simiand, J.; Morre, M.; Dodd, R. H.; Rossier, J. In *Advances in Medicinal Phytochemistry*; Barton, D., Ollis, W. D., Eds.; John Libbey: London, 1986; pp 145–150.
(8) Duka, T. In *New Concepts in Anxiety*; Briley, M., File, S., Eds.; CRC Press: Boca Raton, FL, 1991; pp 440–457.
(9) Matsushita, A.; Kawasaki, K.; Matsubara, K.; Eigyo, M.; Shindo, H.; Takada, S. Activation of Brain Function by S-135, a Benzodiazepine Receptor Inverse Agonist. *Prog. Neuro-Psychpharmacol. Biol. Psychiatry* 1988, *12*, 951–966.

0022-2623/92/1835-4001$03.00/0

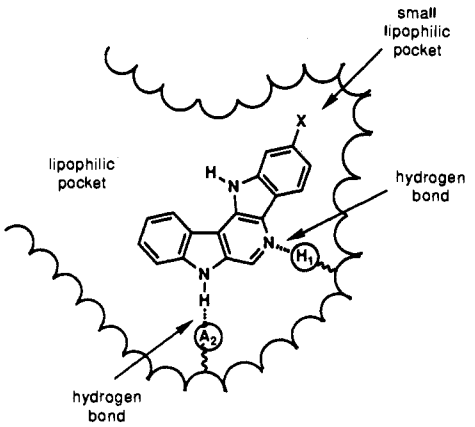

Figure 1. Proposed model of the benzodiazepine receptor inverse agonist/antagonist active site shown with 7,12-dihydropyrido-[3,2-*b*:5,4-*b'*]diindole (IC_{50} = 5 nM) interacting at the hydrogen-bond-donor site (H_1) and hydrogen-bond-acceptor site (A_2) on the binding protein.[15,16,32] The development of the current pharmacophore was based on the template of this rigid and planar BzR inverse agonist.

of barbiturate toxicity have met with limited success. An important advance in this direction came with the recognition that barbiturates bind at or near the chloride ionophore site on the benzodiazepine/$GABA_A$ receptor complex.[10,11] It follows that Bz receptor antagonists or inverse agonists which have an indirect allosteric interaction with the $GABA_A$ receptor and chloride channel may block or reverse the effects of barbiturate toxicity. The BzR inverse agonist 6,7-dimethoxy-4-ethyl-3-carbomethoxy-β-carboline (**3**, DMCM) has been reported to prevent lethality from overdoses of pentobarbital[12] and 3-(hydroxymethyl)-β-carboline (**4**, 3-HMC) reduces pentobarbital-induced decrements in cerebral blood flow and oxygen consumption.[13] The usefulness of βCCM (**2**) and DMCM (**3**) is, however, limited by toxicity and poor (low) water solubility, even as hydrochloride salts. The latter property makes iv administration difficult. Moreover, these compounds are not long-lived in vivo due to rapid esterase-mediated hydrolysis.[14]

In an effort to circumvent the inadequacies inherent in esters **2** and **3**, 3-ethoxy-β-carboline (**5**) was synthesized and proved to be a potent, long-lived, water-soluble partial inverse agonist.[14,15] Its high affinity (24 nM) and in vivo profile are consistent with the previous analysis of the benzodiazepine receptor inverse agonist site[14,15] (see Figure 1). Key features of this model include two hydrogen-bonding interactions. The first is between the indole N(9)-H and a hydrogen-bond-acceptor site (A_2) on the receptor. The second hydrogen-bonding interaction is between the pyridine N(2) nitrogen atom of a β-carboline with a receptor donating site (H_1) on the protein.[14,15]

Recently, we have designed and synthesized new agents to both further test this model and more clearly define the inverse agonist domain of the BzR. This has been accomplished via a three-dimensional quantitative structure–activity relationship (3D-QSAR) analysis of 37 test compounds[16] (cross validated R^2 = 0.59) using the comparative molecular field analysis (CoMFA) approach of Cramer.[17] As a further test of this model, the synthetic method and in vitro binding affinities of a new class of 2-phenyl-2*H*-pyrazolo[4,3-*c*]isoquinolin-3-ols at BzR were determined.[18] The low affinities of these ligands support the previous analysis[14,15] and suggested that a simultaneous interaction at both hydrogen-bond-donor (H_1) and -acceptor sites (A_2) at BzR is required for high-affinity binding of inverse agonists and antagonists. Current research efforts have proceeded to a point where useful predictions of BzR ligand affinities can be made *prior* to the synthesis of the ligands. Described in this report are the predicted affinities of 6 new BzR ligands supported by the subsequent synthesis and in vitro assays of these new agents.

In order to obtain a more robust regression model, we have employed a new procedure termed GOLPE (generating optimal linear PLS estimates).[19-21] It is known that increasing the number of descriptors in a regression equation will improve the fit to a training set of data, but inclusion of too many variables will often cause a substantial reduction in the predictive ability of the model.[22] The technique of partial least squares (PLS)[23] with cross validation as used in CoMFA partially overcomes this problem. However even with this technique, inclusion of irrelevant descriptors will decrease predictive performance as estimated by the cross validated standard error estimate. Moreover, ordinary least squares (OLS) using a limited subset of descriptors has been shown to outperform PLS using a full set of variables as measured by the prediction error sum of squares (PRESS) statistic.[24] In other words, noise tends to obscure signal in PLS analyses. For this reason, it is desirable to include only those variables that are relevant to the prediction. One method that has been used to reduce the number of variables is to exclude those variables which have a low between-molecule variance (e.g.,

(10) Skolnick, P.; Paul, S. M.; Barker, J. L. Pentobarbital Potentiates GABA-Enhanced [^{3}H]-Diazepam Binding to Benzodiazepine Receptors. *Eur. J. Pharmacol.* **1980**, *65*, 125–127.

(11) Ticku, M. K.; Olsen, R. W. Interactions of Barbiturates with Dihydropicrotoxinin Binding Sites Related to the GABA Receptor-Ionophore System. *Life Sci.* **1978**, *22*, 1643–1652.

(12) Havoundjian, H.; Reed, G. F.; Paul, S. M.; Skolnick, P. Protection Against the Lethal Effects of Pentobarbital in Mice by a Benzodiazepine Receptor Inverse Agonist, 6,7-Dimethoxy-4-Ethyl-3-Carbomethoxy-β-Carboline. *J. Clin. Invest.* **1987**, *79*, 473–477.

(13) Albrecht, R. F.; Cook, J.; Hoffman, W. E.; Larscheid, P.; Miletich, D. J.; Naughton, N. The Interaction Between Benzodiazepine Antagonists and Barbiturate Induced Cerebrovascular and Cerebral Metabolic Depression. *Neuropharmacol.* **1985**, *24*, 957–963.

(14) Trullas, R.; Ginter, H.; Jackson, B.; Skolnick, P.; Allen, M. S.; Hagen, T. J.; Cook, J. M. A High Affinity Benzodiazepine Receptor Ligand with Partial Inverse Agonist Properties. *Life Sci.* **1988**, *43*, 1189–1197.

(15) Allen, M. S.; Hagen, T. J.; Trudell, M. L.; Codding, P. W.; Skolnick, P.; Cook, J. M. Synthesis of Novel 3-Substituted β-Carbolines as Benzodiazepine Receptor Ligands: Probing the Benzodiazepine Receptor Pharmacophore. *J. Med. Chem.* **1988**, *31*, 1854–1861.

(16) Allen, M. S.; Tan, Y.-C.; Trudell, M. L.; Narayanan, K.; Schindler, L. R.; Martin, M. J.; Schultz, C.; Hagen, T. J.; Koehler, K. F.; Codding, P. W.; Skolnick, P.; Cook, J. M. Synthesis and Computer-Assisted Analyses of the Pharmacophore for the Benzodiazepine Receptor Inverse Agonist Site. *J. Med. Chem.* **1990**, *33*, 2343–2357.

(17) Cramer, R. D.; Patterson, D. E.; Bunce, J. D. Comparative Molecular Field Analysis (CoMFA). 1. Effect of Shape on Binding of Steroids to Carrier Proteins. *J. Am. Chem. Soc.* **1988**, *110*, 5959–5967.

(18) Allen, M. S.; Skolnick, P.; Cook, J. M. Synthesis of Novel 2-Phenyl-2*H*-Pyrazolo[4,3-c]isoquinolin-3-ols: Topological Comparisons with Analogues of 2-Phenyl-2,5-Dihydropyrazolo[4,3-c]quinolin-3(3*H*)-ones at Benzodiazepine Receptors. *J. Med. Chem.* **1992**, *32*, 368–374.

(19) Cruciani, G.; Baroni, M.; Clementi, S.; Costantino, G.; Riganelli, D.; Skagerberg, B. Prediction Ability of Regression Models, Part I. The SDEP Parameter. *J. Chemometrics* **1992**, in press.

(20) Baroni, M.; Clementi, S.; Cruciani, G.; Costantino, G.; Riganelli, D. Prediction Ability of Regression Models, Part II. Selection of the Best Predictive PLS Model. *J. Chemometr.* **1992**, in press.

(21) Baroni, M.; Cruciani, G.; Costantino, G.; Riganelli, D.; Clementi, S. GOLPE: an advanced chemometric tool for handling 3D-QSAR problems. *Quant. Struct.-Act. Relat.* **1992**, submitted.

(22) Wolde, S. *Quant. Struct. Act. Relat.* **1991**, *10*, 191–193.

(23) Helland, I. S. Partial Least Squares Regression and Statistical Models. *Scand. J. Statist.* **1990**, *17*, 191–193.

(24) Kowalski, K. G. On the Predictive Performance of Biased Regression Methods and Multiple Linear Regression. *Chemometr. Int. Lab. Syst.* **1990**, *9*, 177–184.

Scheme I

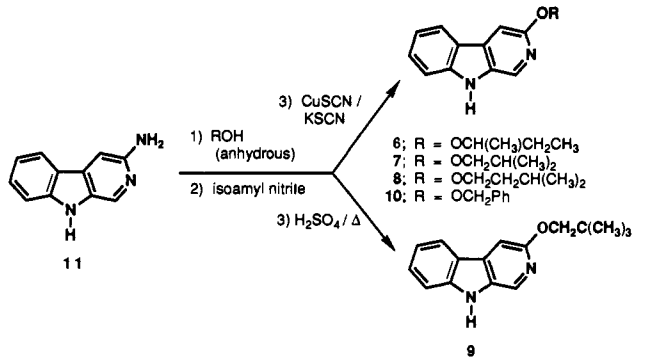

11 9

Scheme II

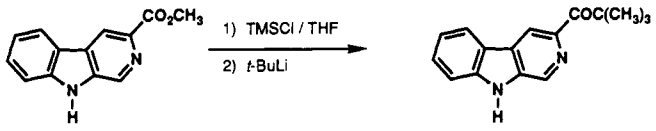

14 12

setting the minimum σ value to a nonzero value in the Sybyl QSAR module). However, this method may retain variables which, despite their high variability between molecules, do not contribute to the predictive ability of the regression equation. Worse yet, other variables which contain useful predictive information may be eliminated owing to low between-molecule variances. As an alternative to the minimum σ variable elimination method, the GOLPE procedure represents an efficient way to identify variables which actually contribute to the predictive ability of the regression equation. Using GOLPE, the previously derived 3D-QSAR regression model was dramatically improved through elimination of irrelevant steric and electrostatic descriptors.

Chemistry

The β-carbolines 6–10 were synthesized to further define the structure–activity relationship (SAR) of the 3-substituted alkoxy-β-carboline derivatives and to refine the receptor model of the lipophilic pocket about position-3 of the bound β-carbolines. The β-carboline 3-alkyl ethers 6–8 and 10 were prepared in a manner similar to that previously reported for the synthesis of 5.[15] In brief, the corresponding diazonium salt of 3-amino-β-carboline (11) was converted into the desired alkoxy derivatives 6–8 and 10 with isoamyl nitrite, a copper(I) salt, and the appropriate anhydrous alcohol at −20 °C (Scheme I), while the 3-neopentoxy derivative 9 was prepared using a modification of the above-mentioned procedure. In the latter case, 3-amino-β-carboline (11) was reacted with isoamyl nitrite, neopentyl alcohol, and concentrated sulfuric acid at 99 °C to generate the 3-neopentoxy analog 9.

1-(9*H*-pyrido[3,4-*b*]indol-3-yl)-2,2-dimethyl-1-propanone (12) was synthesized and screened to further determine the importance of the lipophilic nature of the substituent at the 3-position of a β-carboline. The synthesis was analogous to that of 1-(9*H*-pyrido[3,4-*b*]-indol-3-yl)-1-butanone (13).[16] Briefly, 3-(ethoxycarbonyl)-β-carboline (14) was treated with chlorotrimethylsilane in tetrahydrofuran at −70 °C. The complex which resulted was then treated with *tert*-butyllithium to give *tert*-butyl ketone 12 (Scheme II).

3D QSAR Methods

The coordinates and charges (MNDO[25]//PRDDOE[26])-for the 37 BzR training set ligands were taken from a published work[16] and used as is. The charges used in the initial study were not correct for 3-chloro-β-carboline and ethyl benzothieno[2,3-c]pyridine-3-carboxylate owing to a programming error in a file conversion utility. The charges for these two molecules were corrected in the present work.

The ab initio 3-21G optimizations were performed using the Gaussian-90 program[27] running on a Cray X-MP super computer. The MNDO geometries (see above) were used as the starting point for the ab initio optimizations. All bond lengths and valence angles were optimized while the torsional angles were held fixed. The ab initio optimizations were followed by a single point 6-31G* calculation (SCF=TIGHT convergence criteria). Electrostatic potential fit charges were calculated using the 6-31G* wave function and a program based upon the Kollman et al. algorithm.[28,29]

The CoMFA[17] study was performed using the QSAR option of SYBYL version 5.41c[30] on a Silicon Graphics 4D/35 Personal Iris workstation. Unless specifically stated otherwise, default settings were used throughout. The steric and electrostatic potentials were generated using an sp^3 carbon probe with a 1+ charge. The grid used in the CoMFA study had a resolution of 2.0 Å and the grid dimensions ran from −11.0 to +11.0 Å along the *X* and *Y* axes and from −6.0 to +6.0 along the *Z* axis. These dimensions insured that the grid extended beyond the molecular dimensions by 4.0 Å in all directions and that the Z coordinates of the aromatic rings (0.0 Å) matched exactly the Z coordinate of one plane of the potential grid. The "minimum-sigma" value was set to 1.00. The "QSAR empty-value", "CoMFA switching", and "PLS scaling" tailor options were set to "column-mean", "no", and "none", respectively, in order to more closely reproduce the results of previous versions of Sybyl. Finally, the octanol/water and molar refractivity variables used in the original study were not included in this work since they contributed very little to the overall regression.[16] The potentials used in the GOLPE procedure (see below) were the same potentials used in the CoMFA study and were obtained by capturing to a file the output of the "qsar comfa field extract" followed by "qsar comfa field list" commands in Sybyl.

The identification of regression variables relevant to predictions is a typical statistical design problem. The GOLPE procedure involves six separate steps:[20] (1) derivation of a linear PLS model using all variables, (2) performing a D-optimal design on the PLS loadings to substantially reduce the number of starting variables, identifying the best subset of variables which span the

(25) Dewar, M. J. S.; Thiel, W. MNDO (Modified Neglect of Diatomic Differential Overlap) *J. Am. Chem. Soc.* 1977, *99*, 4899.
(26) Halgren, T. A.; Kleier, D. A.; Hall, J. H., Jr.; Brown, L. D.; Lipscomb, W. N. Speed and Accuracy in Molecular Orbital Calculations. A Comparison of CNDO/2, INDO, PRDDO, STO-3G, and Other Methods, Including AAMON, VRDDO, and ESE MO. *J. Am. Chem. Soc.* 1978, *100*, 6595–6608.
(27) Frisch, M. J.; Head-Gordon, M.; Trucks, G. W.; Foresman, J. B.; Schlegel, H. B.; Raghavachari, K.; Robb, M. A.; Binkley, J. S.; Gonzalez, C.; Defrees, D. J.; Fox, D. J.; Whiteside, R. A.; Seeger, R.; Melius, C. F.; Baker, J.; Martin, L. R.; Kahn, L. R.; Stewart, J. J. P.; Topiol, S.; Pople, J. A. Gaussian 90. Gaussian, Inc., Pittsburgh, PA, 1990.
(28) Besler, B. H.; Merz, J. K. M.; Kollman, P. A. Atomic charges derived from semiempirical methods. *J. Comput. Chem.* 1989, *11*, 431–439.
(29) O'Donnell, T. J.; Spangler, D. P., unpublished results.
(30) Available from Tripos Associates, St. Louis, MO 63144.

"space" of descriptors, (3) performing a fractional factorial design on the remaining variables to obtain a large matrix in which the rows are the "experiments" (i.e., the possible combinations of variables) and the columns represent the presence or absence of variables for each row [For each "experiment" the program evaluates the predictive ability for the actual subset, using the SDEP parameter, where

$$\mathrm{SDEP} = \sqrt{\frac{\sum(Y_{\mathrm{predicted}} - Y_{\mathrm{measured}})^2}{N}}$$

and N = number of predictions.[19]], (4) derivation of a new PLS model in which the SDEP parameters are the regressors and the "design matrix" is the X-block, (5) selecting only those variables which decrease the SDEP parameter, and (6) rederivation of the PLS model using the variables identified in step 5.

The values of steric and electrostatic potentials eliminated by GOLPE were set to zero in the external field file produced by Sybyl. This edited field file was imported back into Sybyl and the minimum σ value was set to 0.01, effectively excluding descriptors set to zero from the analysis.

Results and Discussion

In the 3-substituted alkoxy-β-carboline series, a steady increase in potency is observed as chain length is increased from methoxy (**15**) to ethoxy (**5**) and finally to *n*-propoxy (**16**).[15] However, when the alkyl side chain of 3-*n*-propoxy-β-carboline (**16**) is increased by an additional methylene unit to afford 3-*n*-butoxy-β-carboline (**17**), potency drops off by 1 order of magnitude.[16] Side chains with β- or δ-branching (β-carbolines **18** and **19**, respectively) display a marked decrease in potency compared with their unbranched analogs, while a β-carboline with γ-branching (**20**) displays high affinity[16] (see Table I). These data suggest a lipophilic pocket in the receptor with a well-defined length and width.

To further delineate the dimensions of this lipophilic zone and to more rigorously test our recent model derived from a 3D-QSAR analysis,[16] we predicted the binding affinities of six new 3-substituted β-carboline BzR ligands *before* synthesis was initiated (see Table II). As a test of the predictive ability of our model, these six ligands were then prepared and tested in assays at the BzR in vitro. The results of this work are presented in Table II, which compares the CoMFA predicted vs actual potencies for substituted β-carbolines **6–10** and **12**.

It is apparent from Table II that there is remarkable agreement between the measured binding affinities and those predicted by the original CoMFA regression equation. The experimental uncertainty of the training set pIC_{50} values is on the order of ± 0.2 log units, which places an upper limit on the predictive ability of any regression model derived from this data. A realistic estimate of the error that would be expected for predictions of affinity can be made from the standard error estimate for the training set cross validated runs. In the original study,[16] this estimate of error was 1.0 log units. Surprisingly, the average error between the predicted vs actual binding affinities for the six new ligands **6–10** and **12** is on the order of ± 0.2 log units. This agreement is far better than expected and may simply be a result of chance correlation.

In order to develop a regression model with a smaller estimate of standard error and hence a more credible correlation between measured and predicted binding affinities, the GOLPE procedure was used to reduce the number of variables used in the CoMFA.[19–21] The GOLPE procedure selected 202 out of a possible 2016 electrostatic and steric descriptors. This compares to 217 descriptors selected by Sybyl CoMFA when the minimum σ value is set to 1.00. It should be noted that GOLPE retained some of the potentials that were eliminated by the minimum σ selection method. As can be seen in Table III, there is a substantial improvement in the correlation when the minimum σ selected potentials are replaced with those chosen by GOLPE. The cross validated R^2 increases from 0.65 to 0.82 while the standard error estimate drops from 0.9 to 0.6 log units. In addition, the electrostatic contribution to the regression increases from ~10% to over 50% (see Table IV). This is partially a consequence of the larger percentage of GOLPE selected potentials that are electrostatic (61%) vs minimum σ selected electrostatic potentials (50%). While predictions made using the regression equation derived from GOLPE-selected vari-

Table I. In Vitro Binding Affinity[a] and Inverse Agonist Activity of Selected β-Carboline Ligands to BzR

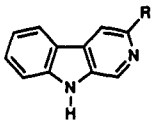

compd	R	in vitro IC_{50}[a] (nM)	in vivo ED_{50} (mg/kg)	in vivo profile
2 (βCCM)	CO_2CH_3	5	10.0[f,g]	convulsant
5	OCH_2CH_3	24[b]	7.0[h]	proconvulsant
6	$OCH(CH_3)CH_2CH_3$	471 ± 23	N/D[f,j]	
7	$OCH_2CH(CH_3)_2$	93 ± 8	N/D[f,j]	
8	$OCH_2CH_2CH(CH_3)_2$	535 ± 84	N/D[f,j]	
9	$OCH_2C(CH_3)_3$	104 ± 34	ND//[j]	
10	OCH_2Ph	>1000	N/D[f,j]	
11	NH_2	>25000	N/D[f,j]	
12	$COC(CH_3)_3$	358 ± 52	N/D[f,j]	
13	$COCH_2CH_2CH_3$	2.8[c]	3.1	proconvulsant
14 (βCCE)	$CO_2CH_2CH_3$	5	3.2[e,g]	proconvulsant/convulsant
15	OCH_3	124[b]	6.0	proconvulsant
16	$OCH_2CH_2CH_3$	11[b]	N/A[k]	antagonist
17	$OCH_2CH_2CH_2CH_3$	98[c]	N/D[f,i]	
18	$OCH(CH_3)_2$	500[c]	N/D[f,j]	
19	$CO_2CH_2C(CH_3)_3$	750	N/D[f,i]	
20	$CO_2C(CH_3)_3$	10	N/A[k]	antagonist
21	$NHCH_2Ph$	>1280[b,d]	N/D[f,i]	

[a] Values for new (previously unpublished) compounds are listed with statistical limits and represent $\bar{X}$ of three or more experiments. [b] See ref 15 for details. [c] See ref 16 for details. [d] 1280 nM at 30% inhibition. [e] See Tenen, S. S.; Hirsch, J. D. β-Carboline-3-Carboxylic Acid Ethyl Ester Antagonizes Diazepam Activity. *Nature* **1980**, *288*, 609–610. [f] N/D = not determined. [g] βCCE is rapidly hydrolyzed in rodents and will cause electroencephalographic but not behavioral seizures, even at very high doses. Since it is so rapidly hydrolyzed, the ED_{50} as a proconvulsant is highly dependent upon both the route of administration and challenge. In squirrel monkeys, where the hydrolysis in plasma has been found to be significantly lower than in rodents, βCCE is a convulsant with an ED_{50} of 0.6 mg/kg. Schweri, M.; Martin, J.; Mendelson, W.; Barrett, J.; Paul, S.; Skolnick, P. Pharmacokinetic and Pharmacodynamic Factors Contributing to the Convulsant Action of β-Carboline-3-Carboxylic Acid Esters. *Life Sci.* **1983**, *33*, 1505–1510. Ninan, P. T.; Insel, T. M.; Cohen, R. M.; Cook, J. M.; Skolnick, P.; Paul, S. M. Benzodiazepine Receptor-Mediated Experimental Anxiety in Primates. *Life Sci.* **1982**, *218*, 1332–1334. [h] Trullas, R.; Ginter, H.; Jackson, B.; Skolnick, P.; Allen, M. S.; Hagen, T.; Cook, J. M. 3-Ethoxy-β-Carboline: A High Affinity Benzodiazepine Receptor Ligand with Partial Inverse Agonist Properties. *Life Sci.* **1988**, *43*, 1189–1197. [i] These ligands have not been screened in vivo to date. [j] Ligands with IC_{50}'s > 200 nM are generally not tested in vivo in this series. [k] N/A = not applicable.

Table II. CoMFA Predicted vs Actual in Vitro Binding of Selected β-Carboline Ligands to BzR

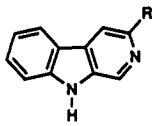

compd	R	actual		predicted		
		IC_{50}[a] (nM)	pIC_{50}[b]	pIC_{50}[b-d]	pIC_{50}[b,c,e]	pIC_{50}[b,d,f]
6	$OCH(CH_3)CH_2CH_3$	471 ± 23	6.33 ± 0.02	6.1	5.5	6.1
7	$OCH_2CH(CH_3)_2$	93 ± 8	7.03 ± 0.04	7.1	7.2	6.8
8	$OCH_2CH_2CH(CH_3)_2$	535 ± 84	6.27 ± 0.06	6.6	6.6	7.0
9	$OCH_2C(CH_3)_3$	104 ± 34	7.02 ± 0.18	6.9	7.1	6.7
10	OCH_2Ph	>1000	<6.00	6.2	4.9	5.6
12	$COC(CH_3)_3$	358 ± 52	6.45 ± 0.06	6.7	6.6	6.2

[a] Values for new (previously unpublished) compounds are listed with statistical limits and represent $\bar{X}$ of three or more experiments. [b] pIC_{50} = -log IC_{50}. [c] Sybyl PLS (minimum σ = 1.00). [d] MNDO//PRDDOE geometries and Mulliken charges. [e] Ab initio 3-21G//6-31G* geometries and ESPFIT charges. [f] GOLPE PLS (see methods section).

Table III. CoMFA Statistics of IC_{50} Data for 37 Benzodiazepine Receptor Ligands

variable selection method	optimal number of components	number of cross validation groups	R^2	standard error estimate	probability $R^2 = 0$
Sybyl[a,b]	4	37	0.65	0.906	0.000
	4	0	0.88	0.536	0.000
Sybyl[a,c]	5	37	0.71	0.814	0.000
	5	0	0.93	0.402	0.000
GOLPE[b,d]	5	37	0.82	0.610	0.000
	5	0	0.92	0.380	0.000

[a] Minimum σ value = 1.00. [b] MNDO//PRDDOE geometries and Mulliken point charges. [c] Ab initio 3-21G//6-31G* geometries and electrostatic potential fit point charges. [d] See methods section.

Table IV. Relative Contributions of Steric and Electrostatic Potentials and Number of Descriptors Used by the CoMFA Regression Equation for Binding Affinity (IC_{50}) to the BzR (n = 37)

variable selection method	relative contributions (number of descriptors[a])		
	steric	electrostatic	total
Sybyl[b,c]	0.893 (109)	0.107 (108)	1.00 (217)
Sybyl[b,d]	0.799 (112)	0.201 (111)	1.00 (223)
GOLPE[c,e]	0.479 (78)	0.521 (124)	1.00 (202)

[a] Out of a possible 7 × 12 × 12 = 1008 steric potentials and 1008 electrostatic potentials for a total of 2016 descriptors. [b] Minimum σ value = 1.00. [c] MNDO//PRDDOE geometries and Mulliken point charges. [d] Ab initio 3-21G//6-31G* geometries and electrostatic potential fit point charges. [e] See methods section.

ables are worse than those obtained from the minimum σ selected descriptors, they are more believable since the cross validated standard error estimate of 0.6 now approaches the average error of prediction of 0.4.

There is overall qualitative agreement between the steric and electrostatic CoMFA maps derived from the minimum σ vs GOLPE-selected potentials (see Figures 2–6); however, there are significant differences as well. In the case of the steric potential maps there is agreement between the unfavorable steric regions; however, the positions of favorable steric regions are markedly different (compare Figures 3 and 5). The favorable steric region seen in the CoMFA map derived from minimum σ potentials (Figure 3) matches closely the position of the presumed hydrophobic pocket in the vicinity of position-3 of the β-carbolines.[16] In the case of the steric map derived from GOLPE-selected potentials, the favorable region is located between receptor sites H_1 and A_2 (see Figure 1) and above the plane of the 7,12-dihydropyrido[3,2-*b*:5,4-*b*']diindole. There is closer correspondence between the electrostatic CoMFA maps (compare Figures 4 and 6). However, in the GOLPE-selected potential map, the region of positive electrostatic potential in the vicinity of receptor site H_1 has been somewhat displaced and a new positive electrostatic region has appeared in the vicinity of the carbonyl carbon in the methyl β-carboline-3-carboxylate (BCCM, **2**). The steric Sybyl CoMFA maps originally derived were previously shown to be in close agreement with excluded volume maps while the electrostatic maps were consistent with the existence of hydrogen-bond-donating and -accepting sites H_1 and A_2, respectively (see Figure 1).[16] The physical significance of the GOLPE-derived steric maps is presently unclear. Because GOLPE employs a D-optimal preselection of variables, variables which are highly collinear are eliminated. If there exists local symmetry across a training set of molecules (for example above and below the plane of the aromatic rings), Sybyl CoMFA will highlight this symmetry. GOLPE in contrast, may only consider one-half of the symmetry-related variables, making the maps sparser and therefore more difficult to interpret.

In order to explore what effect the quality of geometries and charges may have on 3D-QSAR analyses, the study was repeated using ab initio 3-21G//6-31G*//ESPFIT geometries and point charges. The steric (compare Figures 3 vs 7) and electrostatic (Figures 4 vs 8) CoMFA maps are qualitatively very similar. As can be seen in Table III, there is a modest increase in the cross validated R^2 (from 0.65 to 0.71) and a decrease in the standard error estimate (from 0.906 to 0.814). More importantly, the percentage that electrostatics contributes to the regression nearly doubles (see Table IV). One possible explanation why electrostatics have generally played a minor role in 3D-QSAR analyses is that the quality of the charges used (typically Mulliken semiempirical) has been poor. This work clearly demonstrates that using higher quality charges can improve the correlation, hence the use of improved charges should be considered, especially in cases where the electrostatic contribution to the overall regression is low. However the present work also demonstrates that semiempirical geometries and charges in 3D-QSAR analysis may be sufficient for making quantitatively useful predictions.

The synthesis of the 3-*sec*-butoxy-β-carboline (**6**, IC_{50} = 481 nM) was envisioned as a positive control with respect to the 3-isopropoxy analog **18** (IC_{50} = 500 nM). Both the *sec*-butoxy compound **6** and the isopropoxy compound **18** display β-branching and exhibit relatively poor binding affinity. More importantly, when the β-methyl group of **6** is moved to the γ-position of the side chain, the isobutoxy

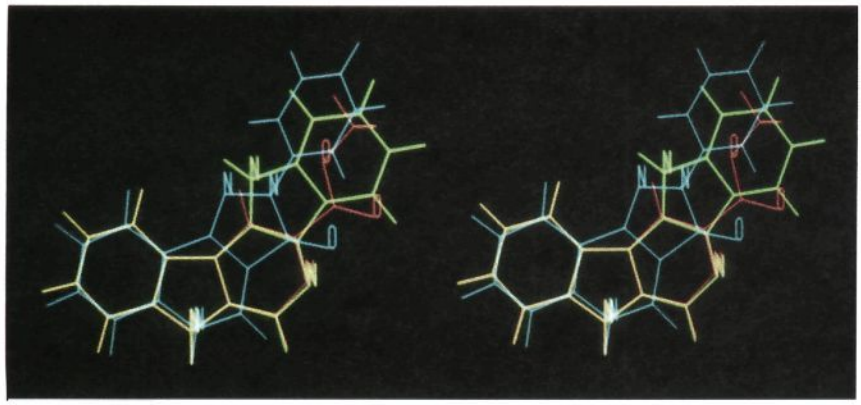

Figure 2. Stereoview of the alignment of methyl 9*H*-pyrido[3,4-*b*]indole-3-carboxylate (BCCM, **2**) (red), 7,12-dihydropyrido[3,2-*b*:5,4-*b*']diindole (green), and 2,5-dihydro-2-phenyl-3*H*-pyrazolo[4,3-*c*]quinolin-3-one (CGS-8216) (blue) used in the 3D-QSAR analysis.

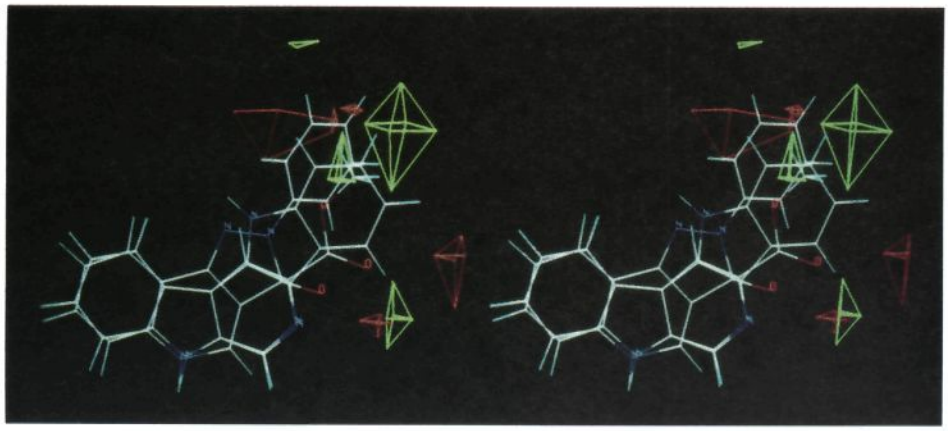

Figure 3. Stereoview of steric CoMFA map based upon MNDO geometries and standard PLS (minimum $\sigma = 1.00$). Green contours surround regions where a higher steric interaction is predicted to increase affinity (the QSAR coefficients times the standard deviation of the corresponding column are greater than 0.10). Red contours surround regions where a lower steric interaction is predicted to increase affinity (less than −0.12). Molecules displayed are the same as in Figure 2.

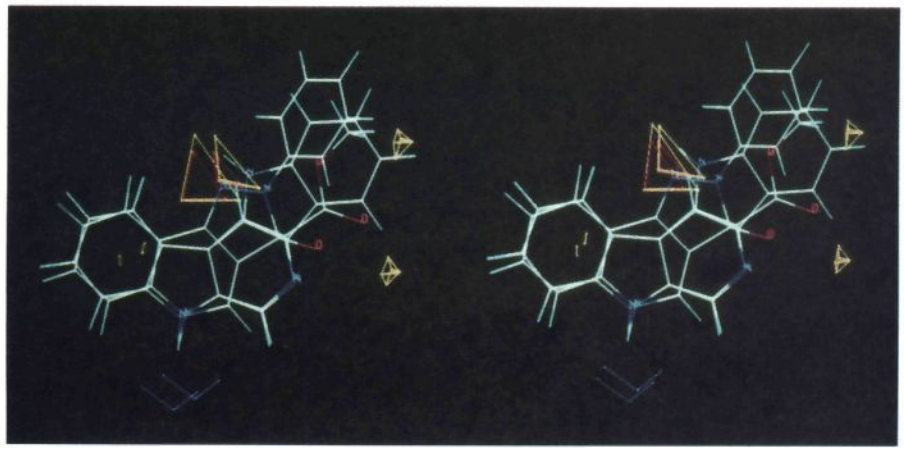

Figure 4. Stereoviews of electrostatic CoMFA map based upon MNDO geometries, PRDDOE Mulliken point charges, and standard PLS (minimum $\sigma = 1.00$). Red and yellow contours surround regions where a more negative electrostatic interaction is predicted to increase affinity (the QSAR coefficients times the standard deviation of the corresponding column are less than −0.030 and −0.015, respectively). Blue contours surround regions where a more positive electrostatic interaction would increase affinity (greater than 0.030). Molecules displayed are the same as in Figure 2.

ligand **7** results, which exhibits enhanced binding affinity (IC_{50} = 93 nM) relative to the *sec*-butoxy compound **6** (IC_{50} = 481 nM). This result is consistent with our previous work[16] and demonstrates that γ-substitution of the alkyl side chain is tolerated without a significant reduction in binding affinity. Addition of an extra methylene unit to the γ-branched 3-isobutoxy derivative **7** (IC_{50} = 93 nM) affords the δ-branched 3-isopentoxy ligand **8** (IC_{50} = 388 nM). This result is again consistent with our previous report which suggests that ligands with δ-branching exhibit a marked decrease in binding affinity relative to their β-branched homologs.[16] This reduction in affinity must be due to δ-branching and not to chain lengthening per se since the unbranched *n*-butoxy derivative **17** (IC_{50} = 98 nM) has a chain length equal to that of branched derivative **8** yet retains relatively high binding affinity.

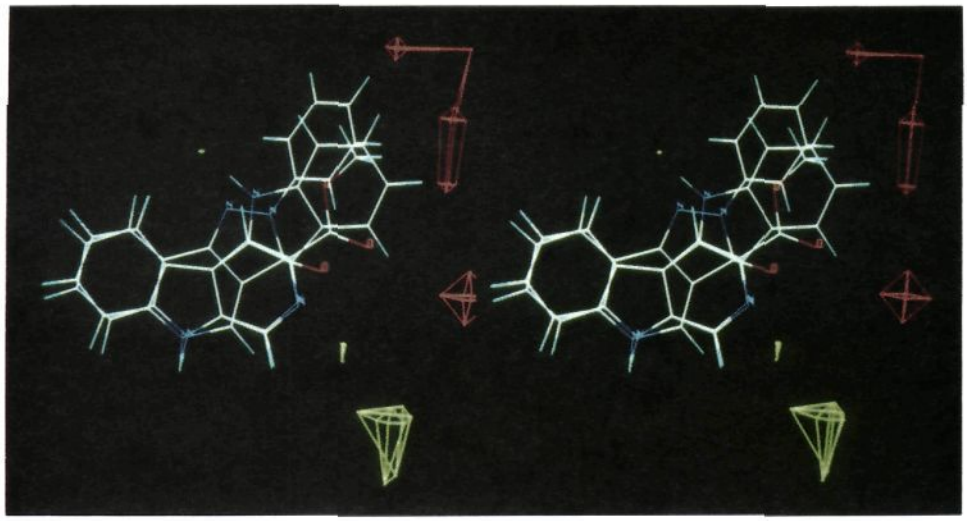

Figure 5. Stereoview of steric CoMFA map based upon MNDO geometries and GOLPE selected potentials. Green contours surround regions where a higher steric interaction is predicted to increase affinity (the QSAR coefficients times the standard deviation of the corresponding column are greater than 0.04). Red contours surround regions where a lower steric interaction is predicted to increase affinity (less than −0.08). Molecules displayed are the same as in Figure 2.

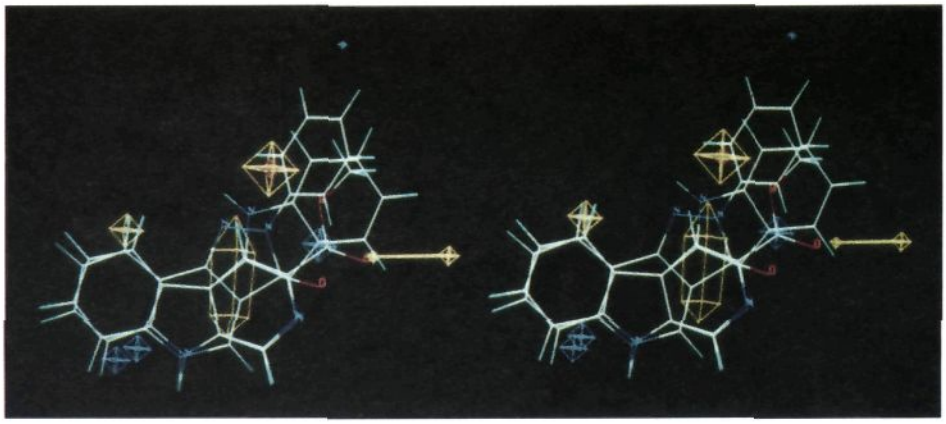

Figure 6. Stereoview of electrostatic CoMFA map based upon MNDO geometries, PRDDOE Mulliken point charges, and GOLPE selected potentials. Red and yellow contours surround regions where a more negative electrostatic interaction is predicted to increase affinity (the QSAR coefficients times the standard deviation of the corresponding column are less than −0.06 and −0.04, respectively). Blue contours surround regions where a more positive electrostatic interaction would increase affinity (greater than 0.06). Molecules displayed are the same as in Figure 2.

Replacement of the methine hydrogen atom of the γ-branched 3-isobutoxy derivative **7** (IC_{50} = 93 nM) with a methyl group provides the doubly γ-branched 3-neopentoxy-β-carboline (**9**, IC_{50} = 104 nM). The neopentoxy ligand **9** was originally prepared as a hydrolytically stable bioisostere of *tert*-butyl ester **20**. The *tert*-butyl ester **20** has been shown to be an important pharmacological tool since it antagonizes the anticonvulsant and antipunishment effects of diazepam.[31] There is only a slight reduction in the potency of **9** compared to **7**, yet **9** is approximately 1 order of magnitude less potent than the isosteric *tert*-butyl ester **20** (IC_{50} = 10 nM). This is probably a result of the smaller valence angle about the β-side chain atom of the ether **9** as compared to the ester **20** (111° vs 131°, respectively; MNDO[25]-optimized geometry). The *tert*-butyl group of the ester **20** is apparently close to an ideal distance from the surface of the lipophilic pocket, which results in a favorable van der Waals attraction. The smaller valence angle of the β-side chain atom of the ether **9** may place the *tert*-butyl group too close to the surface of the binding pocket, resulting in steric repulsion. In addition, the neopentoxy function of **9** has more degrees of freedom and as a result will have a less favorable entropy of binding. Finally, **20** but not **9** can engage in a favorable three-centered hydrogen bond between the 3-carboalkoxy-β-carbolines and the BzR which has previously been shown to enhance binding affinity.[16]

The 3-(benzylamino)-β-carboline (**21**) was previously shown to display low affinity (IC_{30} = 1280 nM).[15] This poor affinity may be a consequence of an unfavorable electrostatic interaction between the aniline hydrogen atom of the ligand and the receptor site H_1. Alternatively, an unfavorable steric interaction between the hydrophobic pocket of the receptor and the benzyl side chain of the ligand may destabilize binding. In order to probe which effect predominates, the isosteric 3-(benzyloxy)-β-carboline derivative **10** (IC_{50} > 1000 nM) was synthesized. Since the replacement of the NH function by an oxygen atom did not significantly enhance binding affinity, it appears

(31) Shannon, H. E.; Guzman, F.; Cook, J. M. β-Carboline-3-Carboxylate-t-Butyl Ester: A Selective BZ1 Benzodiazepine Receptor Antagonist. *Life Sci.* **1984**, *35*, 2227–2236.

(32) Diaz-Arauzo, H.; Koehler, K. F.; Hagen, T. J.; Cook, J. M. Synthetic and Computer Assisted Analysis of the Pharmacophore for the Agonists at Benzodiazepine Receptors. *Life Sci.* **1991**, *49*, 207–216.

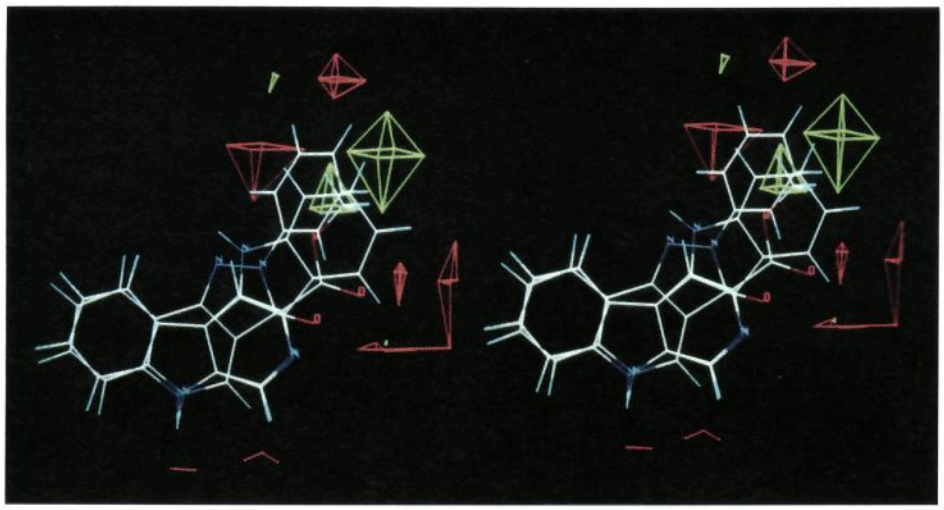

Figure 7. Stereoview of steric CoMFA map based upon ab initio 3-21G geometries and standard PLS (minimum σ = 1.00). Green contours surround regions where a higher steric interaction is predicted to increase affinity (the QSAR coefficients times the standard deviation of the corresponding column are greater than 0.10). Red contours surround regions where a lower steric interaction is predicted to increase affinity (less than −0.12). Molecules displayed are the same as in Figure 2.

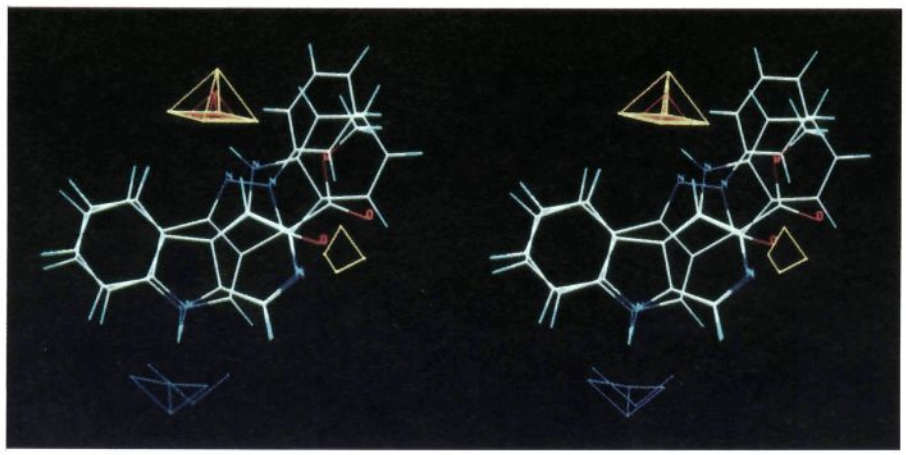

Figure 8. Stereoview of electrostatic CoMFA map based upon ab initio 3-21G geometries, ESPFIT 6-31G* point charges, and standard PLS (minimum σ = 1.00). Red and yellow contours surround regions where a more negative electrostatic interaction is predicted to increase affinity (the QSAR coefficients times the standard deviation of the corresponding column are less than −0.030 and −0.015, respectively). Blue contours surround regions where a more positive electrostatic interaction would increase affinity (greater than 0.030). Molecules displayed are the same as in Figure 2.

that unfavorable steric interactions between the benzyl side chain and the receptor lipophilic pocket are primarily responsible for the low affinity of **21**. The 3-(benzyloxy) analog **10** formally possesses γ-branching and therefore might be expected to share a high affinity with other γ-branched derivatives (e.g., **7** and **9**). However, the length of the 3-(benzyloxy) analog (chain length = 6) appears to be too long to be accommodated by the BzR. This is consistent with previous results[16] which show that there is a marked decrease in binding affinity of 3-substituted straight-chain β-carboline analogs if the chain length is increased beyond four atoms (e.g., compare **16** vs **17**).

As previously mentioned, the 3-(*tert*-butoxycarbonyl)-β-carboline (**20**, IC_{50} = 10 nM) exhibits high affinity binding at the BzR. Removal of the ether oxygen atom of **20** results in the *tert*-butyl ketone analog **12**. This 3-substituted *tert*-butyl ketone derivative **12** (IC_{50} = 358 nM) bears a side chain of the same approximate length as the *n*-propoxy-β-carboline (**16**, IC_{50} = 11 nM) yet it is significantly less potent, even though ketone **12** has the potential of forming a favorable three-centered hydrogen bond with the receptor site (H_1). However, the required s-cis conformation is very strained due to an unfavorable intramolecular steric interaction between the *tert*-butyl group and the hydrogen atom at the 4-position of the β-carboline ring. (The s-cis conformation is calculated to be 10.5 kcal/mol above the s-trans conformation by MNDO[25]). As a result, the ester substituent of β-carboline **12** is probably twisted out of the plane of the ring when bound to the BzR, which weakens the three-centered hydrogen-bonding interaction.

As was previously reported, the potency of the unbranched propyl ketone **13** (IC_{50} = 2.8 nM) retained an extremely high affinity for the receptor protein. In vivo, ketone **13** is a potent partial inverse agonist (ED_{50} = 3.1 mg/kg) and should exhibit a longer duration of action than the isosteric ester 3-(ethoxycarbonyl)-β-carboline (**14**) (IC_{50} = 5 nM). In fact, ketone **13** is nearly twice as potent as ester **14**. Therefore it appears that the ether oxygen atom in 3-carboalkoxy-β-carbolines has little direct effect on affinity or efficacy, other than elongating the side chain by one atom.

The in vitro potency of the 3-substituted alkoxy derivatives increase from methoxy (**15**, IC_{50} = 125 nM) to

ethoxy (**5**, IC_{50} = 24 nM) and finally to *n*-propoxy (**16**, IC_{50} = 11 nM).[15] Moreover, the first two members of this congeneric series are inverse agonists whereas the later analog is an antagonist.[16] The 3-methoxy-substituted derivative **15** (IC_{50} = 125 nM) was recently shown to be a partial inverse agonist (ED_{50} = 6.0 mg/kg) with an ED_{50} lower than that of the long-lived inverse agonist 3-ethoxy-β-carboline (**5**) (see Table I). This result suggests that smaller lipophilic substituents at position-3 which lie close to the plane of the β-carboline ring system tend to be inverse agonists (e.g., **2**, **5**, **14**, **15**), while compounds which carry longer or bulkier substituents at the same position are antagonists (e.g., **16** and **20**). It is possible that favorable steric interactions between substituents at position-3 and the lipophilic pocket are responsible for the antagonist profile of activity for ligands **16** and **20**, since a strong lipophilic interaction in this region may compromise the integrity of the hydrogen bonds between the ligand and receptor at H_1 and A_2 (see Figure 1).

In conclusion, the six new 3-substituted β-carbolines described in this work exhibit a structure–activity relationship that is consistent with that previously reported.[16] More specifically, γ-branched analogs possess significantly higher affinity for the BzR than either β- or δ-branched derivatives. Furthermore, β-carbolines with substituents at position-3 whose chain length is in excess of five atoms display poor affinity. This study also demonstrates that CoMFA is capable of making *quantitatively* useful predictions of binding affinity. The GOLPE procedure, which eliminates irrelevant descriptors from the 3D-QSAR regression equation, was able to substantially increase the cross validated R^2 on the training set of 37 BzR ligands while maintaining a reasonably good prediction of binding affinity for the six new analogs described in this work. Thus, it appears by eliminating irrelevant variables from 3D-QSAR analyses, methods such as GOLPE will become important tools in obtaining regression equations with greater predictive power and should be considered by others engaged in CoMFA studies.

Experimental Section

Receptor Binding. [^{3}H]Diazepam binding to rat cerebral cortical membranes was accomplished using a modification of the method previously described.[11,15] In brief, rats were killed by decapitation, and the cerebral cortex was removed. Tissue was disrupted in 100 volumes of Tris·HCl buffer (50 mM, pH 7.4) with a Polytron (15 s, setting 6–7, Brinkmann Instruments, Westbury, NY) and centrifuged (4 °C) for 20 min at 20000*g*. Tissue was resuspended in a equal volume of buffer and recentrifuged. This procedure was repeated a total of three times and the tissue resuspended in 50 volumes of buffer. Incubations (1 mL) consisted of tissue (0.3 mL), drug solution (0.1 mL), buffer (0.5 mL), and radioligand (0.1 mL). Incubations (4 °C) were initiated by addition of [^{3}H]diazepam (final concentration, 2 mM; specific activity, 76 Ci/mmol, Du Pont-NEN, Boston, MA) and terminated after 120 min by rapid filtration through GF/B filters and washing with two aliquots of ice-cold buffer with a Brandel M-24R filtering manifold. Nonspecific binding was determined by substituting nonradioactive flunitrazepam (final concentration, 10 μM) for the drug solution and represented <10% of the total binding. Specific binding was defined as the difference in binding obtained in the presence and absence of 10 μM flunitrazepam. The IC_{50} values were estimated from Hill plots.

Biological Evaluation of 1-(9*H*-Pyrido[3,4-*b*]indol-3-yl)-1-butanone (13) and 3-Methoxy-β-carboline (15). The proconvulsant actions of **13** and **20** were evaluated in adult (25–30 g), male NIH Swiss mice (Harlan Sprague–Dawley, Frederick, MD). Groups of 6–12 mice were injected (ip) with the test compounds or an equal volume (0.1 mL) of vehicle. Fifteen minutes later, mice were challenged with pentylenetetrazole (PTZ; 0.1 mL; 40 mg/kg in water) and observed for the presence of tonic/clonic convulsions for an additional 15 min. Under these conditions, PTZ did not produce convulsions in vehicle-injected mice. Drugs were dissolved or suspended in 10% diluted Emulphor/90% saline [diluted Emulphor is Emulphor (GAF Corp., Wayne, NJ) diluted 1:1 (w/w) with ethanol]. The proportion of mice exhibiting convulsions at each drug dose was converted to a percentage, and the ED_{50} values were estimated using GraphPad InPlot.

Melting points were taken on a Thomas-Hoover melting point apparatus or an Electrothermal Model IA8100 digital melting point apparatus and are uncorrected. Proton NMR spectra were recorded on a Bruker 250 MHz NMR spectrometer or on a GE 500 MHz instrument. Infrared spectra were recorded with a Beckman Acculab-1 or a Mattson Polaris IR-10400 spectrometer. Mass spectral data (EI/CI) were obtained on a Hewlett-Packard 5855 GC-mass spectrometer, while high resolution mass spectral data were obtained from a Finnigan HR mass spectrometer. Microanalyses were performed on an F and M Scientific Corp. Model 185 carbon, hydrogen, and nitrogen analyzer. Analytical TLC plates employed were E. Merck Brinkmann UV active silica gel (Kieselgel 60 F254) on plastic.

3-*sec*-Butoxy-9*H*-pyrido[3,4-*b*]indole Hydrochloride (6). Isoamyl nitrite (5.0 mL, 48.9 mmol) was added to a stirred solution of 3-amino-β-carboline diacetate (**11**) (0.550 g, 1.8 mmol) in anhydrous 1-methylpropanol (225 mL) and methylene chloride (90 mL) at −20 °C. The mixture was allowed to stir for 45 min, followed by the addition of a solution of potassium thiocyanate (5.4 g, 55 mmol) and copper(I) thiocyanate (3.3 g, 27 mmol) in anhydrous 1-methylpropanol (110 mL) and methylene chloride (55 mL) at −20 °C. The reaction mixture was stirred for 4 h at −20 °C, after which it was allowed to warm to room temperature. The reaction mixture was filtered and the solvent was removed under reduced pressure. The resulting solid residue was dissolved in a aqueous saturated sodium bicarbonate solution (75 mL) and extracted with ethyl acetate (4 × 100 mL). The combined organic layers were dried (Na_2SO_4), and the solvent was removed under reduced pressure. The residue which resulted was purified by flash chromatography (SiO_2, ethyl acetate as eluent) and further converted into the hydrochloride salt by the addition of a solution of ethanol–hydrogen chloride to afford **6** (0.250 g, 58%): mp 178–179 °C; IR (KBr) 3135, 1264, 750 cm^{-1}; ^{1}H NMR (Me_2SO-d_6) δ 1.0 (t, 3 H, *J* = 7.0 Hz), 1.39 (d, 3 H, *J* = 6.0 Hz), 1.7 (m, 2 H), 5.0 (q, 2 H, *J* = 7.0 Hz), 7.28 (t, 1 H), 7.65 (m, 2 H), 8.11 (s, 1 H), 8.36 (d, 1 H), 8.66 (s, 1 H), 11.88 (s, indole, 1 H); MS (CI, CH_4) *m/e* 240 (M + 1). Anal. ($C_{15}H_{16}N_2O$·HCl) C, H, N.

3-Isobutoxy-9*H*-pyrido[3,4-*b*]indole Hydrochloride (7). To a stirred solution of 3-amino-β-carboline diacetate (1.0 g, 3.3 mmol) in anhydrous 2-methyl-1-propanol (375 mL) at −20 °C was added isoamyl nitrite (7.4 mL). The solution was allowed to stir for 6 min, followed by the addition of potassium thiocyanate (10.4 g) and copper(I) thiocyanate (6.7 g) in anhydrous 2-methyl-1-propanol (150 mL) at −20 °C. After 4 h, the reaction mixture was warmed to room temperature. The reaction mixture was filtered and the solvent was removed under reduced pressure. The resulting solid residue was taken up in an aqueous saturated sodium bicarbonate solution (200 mL) and extracted with ethyl acetate (3 × 150 mL). The combined organic portions were dried (Na_2SO_4) and then concentrated in vacuo. The compound was then purified by flash chromatography [SiO_2, ethyl acetate (50%), hexane (50%)]. Upon the addition of a cold saturated ether–hydrogen chloride solution, a precipitate formed which was filtered and washed with cold ether (3 × 20 mL) to provide pure **7** as the hydrochloride salt (0.464 g, 50.9%): mp 222–223 °C: IR (KBr) 1655, 1607, 1431, 1263, 1209, 999 cm^{-1}; ^{1}H NMR (Me_2SO-d_6) δ 1.04 (d, 6 H, *J* = 6.8 Hz), 2.13 (septet, 1 H), 4.17 (d, 2 H, *J* = 6.5 Hz), 7.28 (m, 1 H), 7.62 (m, 2 H), 8.09 (s, 1 H), 8.34 (d, 1 H, *J* = 8.0 Hz), 8.64 (s, 1 H), 10.94 (s, indole, 1 H); MS (CI, CH_4) *m/e* 241 (M + 1). Anal. ($C_{15}H_{16}N_2O$·HCl) C, H, N.

3-Isopentoxy-9*H*-pyrido[3,4-*b*]indole Hydrochloride (8). 3-Amino-β-carboline (**11**), anhydrous 3-methyl-1-butanol, isoamyl nitrite, potassium thiocyanate, and copper(I) thiocyanate were reacted under the analogous conditions employed for the preparation of **7** above to provide **8** (0.438 g, 45.8%): mp 211–

212 °C; IR (KBr) 1655, 1608, 1431, 1264, 1208, 1000 cm^{-1}; ^1H NMR (Me_2SO-d_6) δ 0.97 (d, 6 H, J = 6.5 Hz), 1.73 (d of t, 2 H, J = 6.5 Hz), 1.83 (m, 1 H), 4.41 (t, 2 H, J = 6.5 Hz), 7.28 (m, 1 H), 7.63 (m, 2 H), 8.12 (s, 1 H), 8.34 (d, 1 H, J = 8.0 Hz), 8.65 (s, 1 H), 10.92 (s, indole, 1 H); MS (CI, CH_4) m/e 255 (M + 1). Anal. ($C_{16}H_{18}N_2O$·HCl) C, H, N.

3-Neopentoxy-9*H*-pyrido[3,4-*b*]indole Hydrochloride (9). To a heated and stirred solution of 3-amino-β-carboline diacetate (0.500 g, 1.65 mmol) in anhydrous 2,2-dimethyl-1-propanol (116 g, 95 mL) was added isoamyl nitrite (0.6 mL) and aqueous concentrated sulfuric acid (1.0 mL). The homogeneous solution which resulted was brought to reflux and stirred for 4.5 h, after which it was cooled to room temperature. The solvent was removed under reduced pressure and the residue which resulted was dissolved in an aqueous saturated sodium bicarbonate solution (100 mL) and extracted with ethyl acetate (3 × 125 mL). The combined organic extracts were dried (K_2CO_3) and concentrated in vacuo. The compound was then purified by flash chromatography (SiO_2) with ethyl acetate as the eluent. Upon the addition of a cold saturated ether–hydrogen chloride solution, a precipitate formed which was filtered and washed with cold ether (3 × 10 mL) to provide pure **9** as the hydrochloride salt (0.190 g, 39.7%): mp 246–247 °C: IR (KBr) 1656, 1609, 1431, 1264, 1208 cm^{-1}; ^1H NMR (Me_2SO-d_6) δ 1.07 (s, 9 H), 4.07 (s, 2 H), 7.28 (m, 1 H), 7.61–7.69 (m, 2 H), 8.14 (s, 1 H), 8.36 (d, 1 H, J = 8.0 Hz), 8.66 (s, 1 H), 10.87 (s, indole, 1 H); MS (CI, CH_4) m/e 255 (M + 1). Anal. ($C_{16}H_{18}N_2O$·HCl) C, H, N.

3-(Benzyloxy)-9*H*-pyrido[3,4-*b*]indole Hydrochloride (10). To a stirred solution of 3-amino-β-carboline diacetate (1.0 g, 3.3 mmol) in anhydrous benzyl alcohol (400 mL) at −20 °C was added isoamyl nitrite (7.5 mL). The solution was allowed to stir for 6 min, followed by the addition of potassium thiocyanate (10.4 g) and copper(I) thiocyanate (6.7 g) in anhydrous benzyl alcohol (200 mL) at −20 °C. After 4 h, the reaction mixture was warmed to room temperature. The reaction mixture was filtered and the solvent was removed by Kügelrohr distillation. The residue which resulted was taken up in 200 mL of an aqueous saturated sodium bicarbonate solution and extracted with ethyl acetate (3 × 150 mL). The combined organic portions were dried (Na_2SO_4) and then concentrated in vacuo. The compound was then purified by flash chromatography [SiO_2; ethyl acetate (50%), hexane (50%)]. Upon the addition of a cold saturated ether–hydrogen chloride solution, a precipitate formed which was filtered and washed with cold ether (3 × 20 mL) to provide pure **10** as the hydrochloride salt (0.395 g, 43.7%): mp 198–199 °C; IR (KBr) 1655, 1610, 1420, 1245, 1020 cm^{-1}; ^1H NMR (Me_2SO-d_6) δ 5.46 (s, 2 H), 7.24 (m, 1 H), 7.40 (m, 3 H), 7.52–7.63 (m, 4 H), 7.98 (s, 1 H), 8.28 (d, 1 H, J = 7.9 Hz), 8.59 (s, 1 H), 11.18 (s, indole, 1 H); MS (CI, CH_4) m/e 275 (M + 1). Anal. ($C_{18}H_{14}N_2O$·HCl) C, H, N.

1-(9*H*-Pyrido[3,4-*b*]indol-3-yl)-2,2-dimethyl-1-propanone Hydrochloride (12). To a stirred solution of 3-(ethoxycarbonyl)-β-carboline (14; 1.0 g, 4.17 mmol) in anhydrous tetrahydrofuran (250 mL) under nitrogen at −70 °C was added via syringe neat chlorotrimethylsilane (3.0 mL). *tert*-Butyllithium (1.7 M, 9.0 mL, 3.7 equiv) was then slowly syringed into the reaction mixture with stirring. After the reaction mixture was allowed to stir for 12 h, it was warmed to room temperature. The solution was quenched with the addition of ethanol (5 mL), followed by water (5 mL) and 4 N HCl (20 mL). The solvent was then removed in vacuo and the residue which resulted was brought to pH 8 with a 1 N sodium bicarbonate solution. The aqueous solution was extracted with ethyl acetate (3 × 125 mL), followed by washing of the combined organic portions with a saturated aqueous sodium chloride solution (2 × 100 mL). The organic layer was dried (K_2CO_3) and then concentrated in vacuo. The residue was dissolved in ether (100 mL) into which anhydrous hydrogen chloride was bubbled. The precipitate which formed was filtered, washed with ether (3 × 20 mL), and dried to provide pure **12** as the hydrochloride salt (0.845 g, 70.4%): mp 229–231 °C; IR (KBr) 3275, 1670, 1590, 1380, 1250, 1180 cm^{-1}; ^1H NMR (Me_2SO-d_6) δ 1.48 (s, 9 H), 7.39 (t, 1 H, J = 7.0 Hz), 7.66–7.79 (m, 2 H), 8.60 (d, 1 H, J = 8.0 Hz), 9.11 (s, 1 H), 9.13 (s, 1 H), 10.05 (s, indole, 1 H); MS (CI, CH_4) m/e 253 (M + 1); high-resolution MS m/e 252.1264 ($C_{18}H_{16}N_2O$) requires 252.1262. Anal. ($C_{16}H_{16}N_2O$·HCl) C, H, N.

Acknowledgment. We would like to thank Sergio Cleminti for providing us with an early release of the GOLPE program. We thank T. J. O'Donnell and Dale P. Spangler for making available to us the ESPFIT program. We would also like to thank Richard D. Cramer, David E. Patterson, Kenneth G. Kowaliski, and Richard M. Bittman for helpful discussions and NIMH for financial support (J.M.C.).

Supplementary Material Available: The ab initio optimized coordinates, connection tables, and ESPFIT charges for the 37 molecules in the CoMFA training set and the six new 3-substituted β-carbolines (**6–10** and **12**) (19 pages). Ordering information is given on any current masthead page.